Ott, Jennifer; Pasanen, Toni; Repo, Päivikki; Seppänen, Heli; Vähänissi, Ville; Savin, Hele

Passivation of Detector-Grade FZ-Si with ALD-Grown Aluminium Oxide

Published in:
Physica Status Solidi (A) Applications and Materials Science

DOI:
10.1002/pssa.201900309

Published: 01/09/2019

Document Version
Peer-reviewed accepted author manuscript, also known as Final accepted manuscript or Post-print

Please cite the original version:
Ott, J., Pasanen, T., Repo, P., Seppänen, H., Vähänissi, V., & Savin, H. (2019). Passivation of Detector-Grade FZ-Si with ALD-Grown Aluminium Oxide. *Physica Status Solidi (A) Applications and Materials Science*, *216*(17). https://doi.org/10.1002/pssa.201900309

Passivation of detector-grade FZ-Si with ALD-grown aluminium oxide

Jennifer Ott, Toni P. Pasanen, Päivikki Repo, Heli Seppänen, Ville Vähänissi, Hele Savin*

J. Ott
Helsinki Institute of Physics, Gustaf Hällströmin katu 2, FI-00014 University of Helsinki, Finland
Aalto University, Department of Electronics and Nanoengineering, Tietotie 3, FI-02150 Espoo, Finland
E-mail: jennifer.ott@aalto.fi

T. P. Pasanen, Dr. P. Repo, H. Seppänen, Dr. V. Vähänissi, Prof. H. Savin
Aalto University, Department of Electronics and Nanoengineering, Tietotie 3, FI-02150 Espoo, Finland

Keywords: detectors, float-zone silicon, aluminium oxide, surface passivation, charge carrier lifetimes

Silicon radiation and particle detectors are traditionally passivated with thermal silicon dioxide. It has been shown that aluminium oxide (Al_2O_3) films provide better surface passivation due to their high negative charge, but studies on Al_2O_3 surface passivation are usually performed on low-resistivity substrates. In this article, the passivation of high-resistivity, detector-grade float-zone silicon with Al_2O_3 is studied, with a specific emphasis on the effect of post-anneal temperature on carrier lifetimes and film properties. It is confirmed that Al_2O_3 provides excellent surface passivation also on high-resistivity FZ-Si substrates, with a low interface defect density of around $(2\text{-}4)\times10^{11}$ $cm^{-2}eV^{-1}$ and high negative oxide charge of 1×10^{12} to 3×10^{12} q cm^{-2} , when post-annealed at temperatures of up to 450-500 °C. In addition, high-resistivity samples are studied for the phenomenon of bulk lifetime degradation occurring at typical post-anneal or metal sintering temperatures, which has been reported for low-resistivity FZ silicon. At post-anneal temperatures of >500 °C, reduced bulk lifetimes are observed if the substrates did not receive high-temperature treatment prior to surface passivation. Furthermore, it is noticed that n-type samples exhibit lower bulk lifetimes even when a high-temperature treatment was performed, which indicates a connection between FZ-Si bulk lifetime degradation and doping type.

1. Introduction

Silicon is used in a variety of semiconductor radiation and particle detectors due to its reasonable cost, good availability and processability, and performance at room temperature. High bulk resistivity (≥ 1 kΩcm) silicon is preferred for detector applications, as it allows full or at least partial depletion of the device from the p-n junction, which is needed to reduce background noise. In addition to the resistivity, the other critical factor for detector material is the recombination lifetime of minority charge carriers in the silicon bulk, as trapping or recombination of charge carriers before they are collected at the electrodes is directly linked to loss in detection efficiency. While specific impurities such as carbon and oxygen may increase silicon radiation hardness, they also play a role in the trapping or recombination of charge carriers leading to decreased carrier lifetimes and lower signals, and are thus usually unwanted in the substrate.[1-4] The starting material that best meets the aforementioned criteria is float zone (FZ) silicon, which is thus the most common substrate material used in silicon radiation and particle detectors.[5-7]

Even more significantly than bulk defects, bare silicon surfaces in a device offer a large number of possible defect sites for charge carrier recombination, and therefore need to be passivated. In detectors, such surface passivation is traditionally realized by thermally grown silicon dioxide (SiO_2) that is known to form a high-quality interface on silicon and additionally provides good electrical insulation. Optimization of SiO_2 passivation is mainly achieved by tuning the post-oxidation annealing step, e.g. by a so-called al-neal, which enhances the neutralization of interface defects through the introduction of hydrogen.[8] However, SiO_2 has only a low, positive oxide charge, which does not provide optimal field-effect passivation.[9,10] Furthermore, in devices with electron-collecting electrodes, a positive oxide charge even leads to the formation of interconnecting channels between electrodes and therefore loss of spatial resolution, or even short-circuiting.

A solution to the above problems could be provided by aluminium oxide (Al_2O_3) thin films, which are known to have a relatively high, negative oxide charge.[11,12] If Al_2O_3 is deposited by atomic layer deposition (ALD), the interface with silicon is of high quality, and thus efficient surface passivation can be reached.[13-15] An additional benefit is that ALD-Al_2O_3 films can be deposited at very low temperatures (< 300 °C), as compared to high-quality thermal SiO_2 at >1000 °C, although Al_2O_3 films require a post-deposition anneal at slightly higher temperature (~400 °C) in order to „activate" the passivation.[14-16] In device processing, however, this activation anneal can often be combined with other process steps that are performed in a similar temperature range, an example being the sintering of the metal contacts. ALD-Al_2O_3 film thus saves processing time and greatly reduces the thermal budget of the devices. Due to the combination of these advantageous properties, ALD-Al_2O_3 films have recently become a common surface passivation dielectric in silicon photovoltaics.[17]

Some promising demonstrations of Al_2O_3 surface passivation exist already for photodiode and particle detector applications, but thermal SiO_2 still dominates in the detector industry.[18,19] This is probably because in the case of high-resistivity silicon, very little has been presented about the properties of Al_2O_3 films and the interface with silicon under different processing conditions, as the majority of studies on Al_2O_3 surface passivation are focusing on low-resistivity substrates for photovoltaic applications. The abovementioned publications on detector applications also did not include further optimization of the Al_2O_3 process specifically for their purpose. Most importantly, the optimization requires assessing the effect of post-annealing parameters, foremost annealing temperature, on the Al_2O_3 passivation. Related to the ALD post-anneal, it is also important to study whether the specific recombination-active defect that has been reported to appear in low-resistivity FZ-Si in temperatures between 400 and 800 °C is present also in high-resistivity FZ-Si. [20-22]

This defect is known to anneal out using a high-temperature treatment above 800-1000 °C, and thus has not been reported in detectors in which high temperature thermal SiO_2 passivation is used. This defect may become a problem if SiO_2 is replaced by low-temperature ALD Al_2O_3.

In this contribution, we compare the surface passivation properties of both p- and n-type high-resistivity FZ-Si substrates by ALD-grown aluminium oxide with conventional thermal SiO_2. In order to optimize the ALD Al_2O_3 passivation properties for detector wafers, a special focus is placed on the evolution of effective charge carrier lifetime and electrical properties of ALD-Al_2O_3 passivation layers with post-deposition anneal temperature and comparison of the results with the existing data available for low-resistivity silicon. Finally, we investigate whether the lifetime-degrading bulk defect that has been observed in low-resistivity FZ-Si manifests also in high-resistivity substrates, and if it can be neutralized by the same method as is used by the photovoltaic community.

2. Experimental Section

2.1 Sample preparation

Our experiments were performed on high-resistivity (>10 kΩcm) high-purity float-zone silicon (HPS) wafers obtained from Topsil, doped either with boron (p-type) or phosphorus (n-type) during crystal growth. For both dopant types, the wafer diameter was 100 mm, thickness 525 µm and crystal orientation <100>. A schematic visualizing the sample preparation and characterization flow is presented in Figure 1.

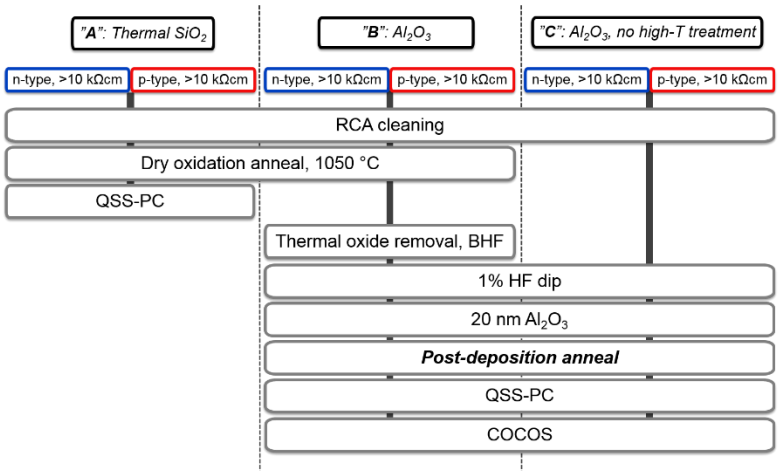

Figure 1. Fabrication and characterization sequence for samples with SiO_2 passivation (left, "A"), Al_2O_3 passivation (center, "B"), and references without high-temperature step (right side, "C") before Al_2O_3 deposition and post-deposition anneal.

All wafers were first subjected to a standard RCA cleaning sequence, consisting of 10 min cleaning in an SC1 solution, a 2 min dip in 1 % HF, and 15 min cleaning in an SC2 solution. After this, one wafer of each doping type was set aside for reference, while the others were again RCA-cleaned with an HF dip as final step, and subsequently oxidized in dry oxidation conditions in a Centrotherm E1200HT 260-4 quartz tube furnace at 1050 °C for 30 min to grow a thermal SiO_2 layer for surface passivation, while simultaneously deactivating the lifetime-degrading bulk defect in FZ-Si. The resulting oxide thickness was measured to be 55 nm by ellipsometry.

After measuring the carrier recombination lifetimes of the aforementioned SiO_2-passivated samples (series "A"), the thermal oxide was removed by wet etching in buffered hydrofluoric acid (BHF), and the wafers were joined for ALD-Al_2O_3 deposition (series "B") with the references that had not received the high-temperature anneal (series "C").

The wafers were subsequently cleaved in quarters. Immediately prior to Al_2O_3 deposition, a 2 min dip in 1 % HF was performed on all samples in order to obtain a hydrophobic surface.

Al_2O_3 deposition was performed in a Beneq TFS-500 batch-type ALD reactor at 200 °C. Samples were coated in groups of four, keeping the process parameters constant between individual deposition runs.

One ALD cycle consisted of a double pulse of 200 ms + 200 ms trimethylaluminium (TMA), followed by a 7 s N_2 purge, then a 250 ms + 250 ms double pulse of DI water, and another final 7 s N_2 purge. This sequence was repeated 200 times, resulting in a film thickness of 22 nm as determined by ellipsometry.

Post-deposition annealing of the Al_2O_3 films on sample series "B" and "C" was done in a PEO-601 quartz tube furnace in nitrogen atmosphere. In order to investigate the effect of post-anneal temperature on film properties and the substrate bulk in a temperature range typical for e.g. metal contact sintering, samples were annealed at different temperatures between 450 and 600 °C. As the post-deposition anneal time for Al_2O_3 surface passivation layers is often reported with 30 min, and on the other hand it has been shown in the case of SiO_2/Al_2O_3 stacks that even a 50 °C increase in annealing temperature to 450 °C reduced the required anneal time to <10 min, annealing times of 30 min at 450 °C and 15 min at 500 °C were chosen here.[11,16,23] To limit the effects of the heat ramping compared to the actual anneal, annealing times were shortened only to 12 min at 550 °C and 10 min at 600 °C, respectively.

2.2 Characterization

Charge carrier lifetimes as a function of minority carrier density were measured by quasi-steady-state photoconductance (QSS-PC) with a Sinton Instruments WCT-120TS tool at room temperature. The measurements represent the carrier lifetime in an area of approximately 2 cm in diameter at the center of the sample.

In order to separate effective lifetime degradation due to bulk defects from surface recombination components caused by possible degeneration of the Al_2O_3 passivation layer, injection-dependent lifetime data was fitted with a model containing both bulk and surface recombination parameters as described by Nampalli *et al*.[24]

An Auger component was adapted from Richter *et al*.[25,26] Additional SRH defect levels introduced or deactivated by high-temperature thermal treatment were not modeled individually, but their effect was included in the lifetime's bulk component.

A profile of the uncertainties in the injection-dependent lifetime measurement was created by repeating the measurement of the same sample several times and determining the deviations of the results at a given injection level. The best fit of the model to the experimental data was chosen as the parameters minimizing χ^2 based on the aforementioned error profile.

Total oxide charge (Q_{tot}) and interface defect densities (D_{it}) were determined by the corona oxide characterization of semiconductors (COCOS) method, using a Semilab SDI PV-2000 Lifetime Scanner.[27]

D_{it} values are represented as values at mid-gap, calculated with a doping concentration of 1.3×10^{12} cm^{-3}. Errors are given as standard deviations from an average of three measurements on each sample.

3. Results and Discussion

3.1. Comparison of Al_2O_3 and thermal SiO_2 surface passivation

A comparison of injection-dependent lifetimes in sample series "A" passivated by thermal SiO_2 and sample series "B" passivated with an ALD Al_2O_3 layer is shown in Figure 2. Carrier lifetimes in Al_2O_3-passivated samples are very high for both n- and p-type substrates.

Assuming infinite bulk lifetime, the effective lifetime values of 10.5 and 7.3 ms at an injection level of 1×10^{15} cm^{-3} correspond to effective surface recombination velocities of 3.6 and 2.5 cm s^{-1} for p- and n-type substrates, respectively. This demonstrates excellent surface passivation for both substrate types, which is expected to considerably improve device efficiency in a detector. The lower effective lifetime in the p-type substrate may be influenced by the increased impact of recombination-active defects (such as iron) compared to phosphorus-doped Si, or can be due to the different amount of defects present in the different ingots. [28,29]

Surface passivation provided by SiO_2 is clearly inferior compared to post-annealed Al_2O_3: effective lifetimes are only around 1.3 ms and thus clearly lower than lifetimes achieved by Al_2O_3 passivation. Since the bulk quality is identical to the Al_2O_3-passivated samples, lifetimes in SiO_2-passivated samples are limited by surface recombination, not bulk recombination, as also indicated by an effective surface recombination velocity of 19.9 cm s^{-1}. Consequently, SiO_2 passivation is also not able to bring out differences in n- and p-type bulk recombination.

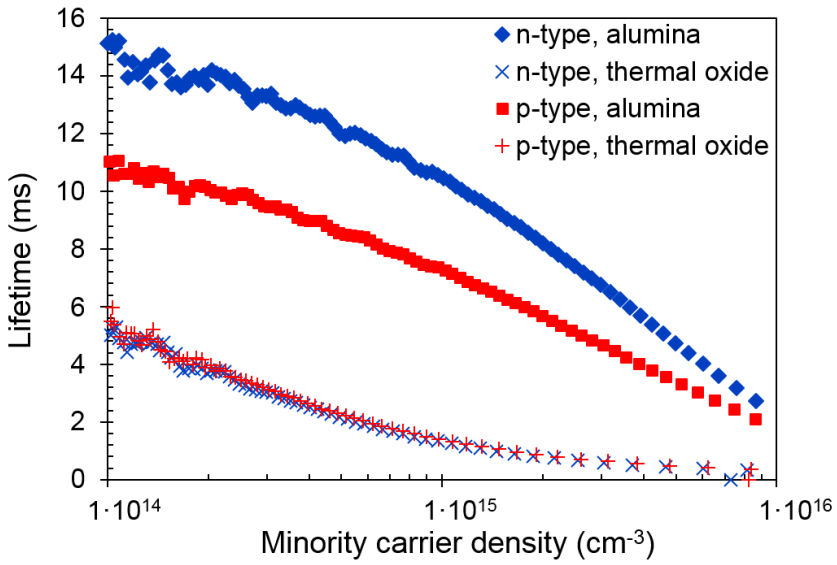

Figure 2. Effective lifetimes of n- and p-type FZ-Si samples passivated with 20 nm ALD-Al_2O_3 and annealed at 450 °C, as compared to 50 nm of thermal SiO_2 obtained in oxidation at 1050 °C.

The effective surface passivation provided by Al_2O_3 is known to include contributions from both chemical passivation, and field-effect passivation due to a high charge at the oxide layer. Chemical passivation with Al_2O_3 is provided by the diffusion of hydrogen to the Si-Al_2O_3 interface during post-deposition annealing, and the resulting termination of dangling bonds and passivation of defects, which would otherwise act as recombination centers for charge carriers.[12,16, 23] Direct effusion of hydrogen out of the system is prevented by the Al_2O_3 film, which acts as an efficient outgassing barrier.[17] In the case of SiO_2, hydrogen would need to be supplied externally through a layer of temporary Al metallization or the annealing ambient.[8]

The origin of a high negative charge at the Si-Al_2O_3 interface has been linked primarily to the non-stoichiometric composition of the film in the very first layers, with an excess of oxygen from –OH bonds providing a net negative charge within 1-2 nm off the interface.[11,12] This is enhanced by a thin (~0.5 nm) SiO_x interfacial layer formed between Si and Al_2O_3 even after a pre-deposition HF dip, which increases the effective negative charge by its higher content of oxygen.[13,30,31] Stoichiometric SiO_2, on the other hand, exhibits a weak, positive charge.[9,10] It is worth to note that in lifetime studies where bulk recombination phenomena are being investigated, SiO_2 passivation is often examined after the addition of corona charge on the oxide surface in order to enhance passivation by the electric field effect, for which the intrinsic charge of thermal SiO_2 is not sufficient.[32-34] This approach is straightforward and does achieve good surface passivation, but it does not correspond to the passivation provided by SiO_2 in realistic device processing conditions. Here, charge carrier lifetimes in the SiO_2-passivated wafers were measured without additional corona charge, mimicking an actual device fabrication process, where the addition of external charge would not be feasible.

To summarize, the efficient surface passivation provided by Al_2O_3, without requiring a post-deposition anneal under metallization or forming gas atmosphere or addition of artificial corona charge, make this material a serious alternative to SiO_2 as passivation dielectric for both n- and p-type Si substrates in detector applications.

In the following section, the evolution of lifetime and interface properties of Al_2O_3 passivation with post-deposition anneal temperature is studied in more detail.

3.2. Effect of post-anneal temperature on Al2O3 passivation

After having demonstrated that Al_2O_3 provides superior surface passivation in terms of effective lifetimes compared to thermal SiO_2 in detector processing conditions, we now study the passivation properties of Al_2O_3 on sample series "B" in more detail. We focus on temperatures starting at 450 °C, which are typical temperatures for metal contact sintering in detector processes, and investigate if surface passivation is retained also at higher temperatures.

Figure 3 visualizes the impact of post-deposition anneal temperature on the effective lifetimes (a) and lifetime surface component extracted by modelling (b) in Al_2O_3-passivated samples at temperature range between 450-600 °C. Lifetimes are reported at an injection level of 1×10^{15} cm^{-3}, due to easier comparison with results in the literature, as well as the limited accuracy of the injection-dependent measurements at very low minority carrier densities ($< 1\times10^{13}$ cm^{-3}). Between 450-500 °C, essentially no change in effective lifetime is seen for p-type, and also the decrease in lifetime for n-type is small. After 500 °C, a clear decrease in effective lifetimes is observed for both p- and n-type samples, however less strongly in the case of p-type than n-type samples. It is observed that even when annealed at 600 °C, effective lifetimes remain higher for Al_2O_3-passivated samples than in the SiO_2-passivated samples.

Surface lifetimes also decrease towards higher temperatures, but especially for n-type samples, they do not obey the exact same trend as the corresponding effective lifetimes, indicating that changes occur also in the bulk, which are discussed further in Section 3.3.

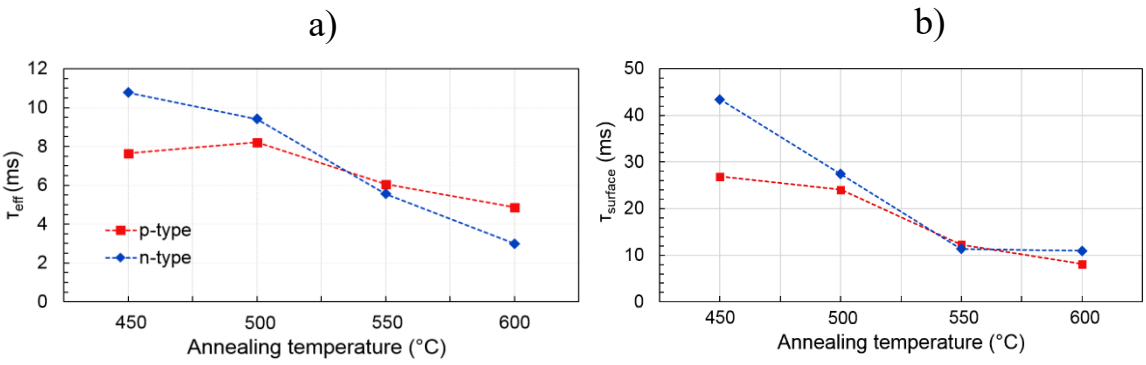

Figure 3. Effective lifetimes and surface recombination lifetimes of n- and p-type FZ-Si samples at different activation anneal temperatures of the ALD-Al_2O_3 passivation.

The observed decrease in carrier lifetimes is in good agreement with the literature for low-resistivity samples passivated with Al_2O_3 films deposited under similar conditions, which mentions deterioration of surface passivation in terms of effective lifetimes or surface recombination velocity $S_{eff,max}$ with increasing post-anneal temperature.[16] Notably, this is occurring here at a higher temperature, > 500 °C, whereas in most earlier studies, a reduction in lifetime has been observed already above 400 °C.[14,16,17] However, even for low-resistivity substrates an optimal temperature of 470 °C has been reported in one other case, which also suggests the possible retention of good surface passivation up to higher temperatures around 500 °C, as was observed here.[35]

It is worth remembering that the surface recombination velocity $S_{eff,max}$ is often determined directly from lifetime spectroscopy data, under the assumption that bulk lifetime is infinite. As discussed further in section 3.3, this assumption may lead to incorrect conclusions about surface passivation, in case bulk lifetimes are also decreasing upon annealing. Therefore, the D_{it} is used here as the primary means to describe the interface quality in terms of defect density.

Here, the COCOS method was employed to study oxide charge and interface defect density of the Al_2O_3 layer itself as a function of post-deposition anneal temperature (Figure 4), to search for correlations with the observed surface lifetimes.

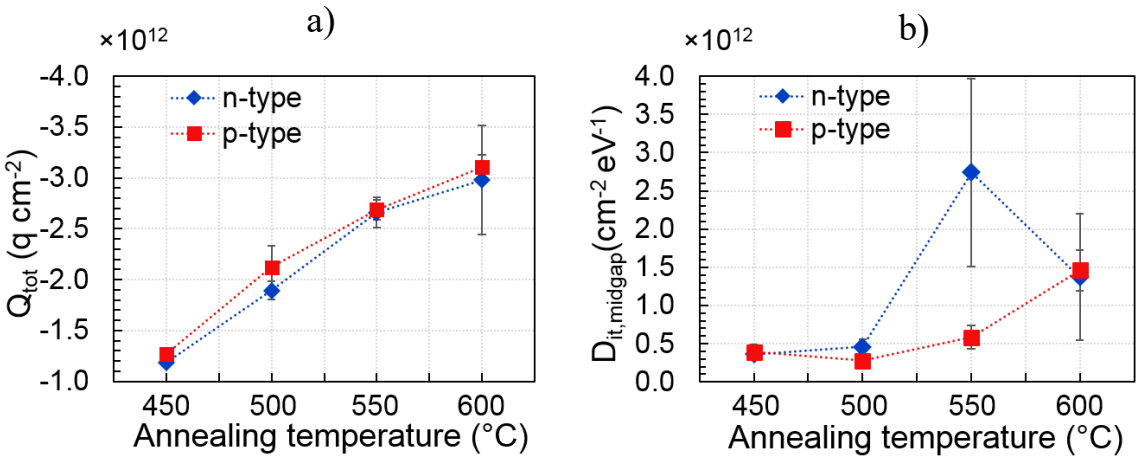

Figure 4. Total negative charge (Q_{tot}) and interface defect density (D_{it}) values at different post-deposition anneal temperatures for n- and p-type FZ-Si samples passivated with ALD-Al_2O_3.

The total negative oxide charge (Q_{tot}) of the Al_2O_3 film was found to increase with increasing annealing temperature (Figure 4a) over the whole range of studied post-anneal temperatures, from around 1×10^{12} q cm^{-2} to 3×10^{12} q cm^{-2}. These values correspond well to current knowledge on oxide charges of Al_2O_3 films, especially such deposited with H_2O as oxidant, which tendencially leads to lower oxide charges than O_3.[11,12,14,15] Regardless of post-anneal temperature, the charge of Al_2O_3 is significantly higher than would be the case for thermal SiO_2 (with typical positive charge values reported at around 1×10^{11} cm^{-2}).[34,36] Thus, Al_2O_3 should provide efficient field-effect passivation of both p- and n-type Si surfaces without any other treatment than the post-deposition anneal.

The continuous increase of Q_{tot} with increasing post-anneal temperature observed here does not support models that suggest the effective charge at the Si-Al_2O_3 interface to be essentially constant at post-anneal temperatures at 400 °C and above.[17]

For Al_2O_3 films deposited by plasma-enhanced ALD, the effective charge has indeed been reported to remain constant - or even slightly decrease - with annealing temperature.[17,37,38] Studies on films deposited by thermal ALD, however, report an increase of the negative charge up to at least 450 °C with H_2O as oxidant, or up to 500 °C with O_3 oxidant.[35,38] To these, the results obtained here provide confirmation and complementation by the extension of measurements towards higher post-anneal temperatures. It is concluded that the behavior of Q_{tot} with annealing temperature is determined by changes of the Si-Al_2O_3 interface, which are discussed in more detail below also in connection with the D_{it}. These properties in turn are influenced primarily by the choice of ALD process and oxidant, as well as potential surface pre-treatments. No significant effect can be attributed to substrate resistivity.
Furthermore, p- and n-type samples do not exhibit differences in absolute Q_{tot} nor its behavior with post-anneal temperature; thus at least in low concentrations, doping does not impact field -effect passivation.

The interface defect density (D_{it}, Figure 4b) at the Al_2O_3-Si interface was measured to be (2-4)×10^{11} $cm^{-2}eV^{-1}$ at 450-500 °C. These values are comparable to results obtained typically for Al_2O_3 and Al_2O_3/SiO_2 on substrates with lower resistivity, which are reported with ~ 1×10^{11} $cm^{-2}eV^{-1}$ at minimum, and confirm that a good-quality interface with high-resistivity FZ-Si by can be obtained by Al_2O_3. [11-13,16] As the post-anneal temperature is increased to 550 and further to 600 °C, the D_{it} increases clearly towards > 1×10^{12} $cm^{-2}eV^{-1}$. Apart from a potentially anomalous measurement point in n-type at 550 °C, the D_{it} for p- and n-type samples behaves in a very similar fashion.

In earlier studies investigating the surface passivation with Al_2O_3 in terms of $S_{eff,max}$ and/or effective lifetimes, passivation quality has been found to peak at 400 °C and decrease above that for both thermal and plasma-enhanced ALD, which has likely contributed to establishing

temperatures around 400-425 °C for the Al_2O_3 activation anneal.[14,16] Instead, a less clear picture is obtained when examining the D_{it}: for thermal ALD, it has been reported to decrease continuously up to 450 °C (H_2O oxidant) and even 600 °C (O_3 oxidant); or to increase from 400 to 500 °C (H_2O oxidant), which is again more in line with observations using $S_{eff,max}$.[23,35,38]

Similarly to above in the case of Q_{tot}, also the D_{it} and its behavior with temperature appears to be mostly determined by the ALD process parameters, here also specifically the choice of oxidant. Results obtained here for high-resistivity substrates do not clearly deviate from observations on low-resistivity substrates, and appear to align with other reports on thermal ALD processes using H_2O as oxidant.

The trend in D_{it} evolution with increasing post-anneal temperature supports the observation of reduced surface passivation quality, as already indicated above in Figure 3b in terms of decreased surface lifetimes. This shows that at the presence of a strong field-effect passivation component, caused by the high negative charge of Al_2O_3 as described above, surface passivation is ultimately limited by chemical passivation of the interface, and the decrease in effective lifetimes correlate with an increase in D_{it}. In other words, above a certain level (as also mentioned in the literature as ~10^{12} q cm^{-2}), even a further increase in Q_{tot} with post-anneal temperatures does not provide an improvement to effective lifetimes, if simultaneously the chemical passivation is degraded.[17]

We attribute the inferior interface quality with increasing post-anneal temperatures, observable as an increase in D_{it}, to the desorption of hydrogen from defect sites and enhanced effusion through the Al_2O_3 layer. This is supported by earlier findings, which show that at higher temperatures, the concentration of hydrogen at the interface is reduced.[23] The increase in Q_{tot} in turn may then be explained by the net negative charge of some re-activated defects, or the introduction of new ones, e.g. interstitial hydrogen acting as an electron trap.[11]

Also the tetrahedral coordination of Al close to the interface, as opposed to octahedral coordination in the film itself, has been proposed as a contribution to the negative charge.[11,13] However, several studies with x-ray photoelectron spectroscopy could not observe a significant difference in the Al signals before and after annealing, which indicates that not Al coordination per se, but rather the amount of oxygen and the configuration of its bonds, is the dominant factor in the development of the Al_2O_3 interface charge.[23,31,39,40]

Another property with may be affected by the post-deposition anneal is the density of the Al_2O_3 film. The densification of Al_2O_3 thin films upon annealing, in association with shrinking, i.e. decrease in measured film thickness, has been investigated in earlier reports; however, these changes were found to be very small (< 5 %) at 600 °C.[40,41] The onset of crystallization of Al_2O_3 reportedly only occurs at even higher temperatures above 800 °C.[40] Similarly, an enhanced growth of silicon oxide at the interface upon annealing does not occur yet at 600 °C.[39,41] Therefore, it is unlikely that changes in D_{it} and Q_{tot} in the temperature range studied here can be explained by changes in film stoichiometry.

3.3 Effect of high-temperature treatment

As shown by our results presented above, Al_2O_3 provides good-quality surface passivation in a wide range of post-deposition anneal temperatures up to 500 °C. However, at least low-resistivity FZ-Si has been reported to suffer from reduced bulk lifetime as a consequence of the formation of a defect during annealing at lower temperatures, when it has not been previously subjected to a high-temperature anneal at > 1000 °C. So far the focus of deeper investigation has been on the role of nitrogen impurities in silicon, on FZ-Si bulk lifetime degradation, and it therefore cannot be excluded that high-resistivity detector-grade FZ-Si substrates may also be affected by this phenomenon [20, 42]. Consequently, we investigate the effect of high-temperature treatment on bulk lifetimes by comparing sample series “B” and “C”.

Bulk lifetimes calculated with the method described in section 2.2 are shown in Figure 5 as a function of post-anneal temperature for p- and n-type samples with and without a high-temperature treatment for curing the defect prior to surface passivation. Similar to reports for low-resistivity substrates, bulk lifetimes are degraded from 500 °C onwards in the samples which had not experienced the high-temperature treatment. The same phenomenon is observed regardless of dopant type.

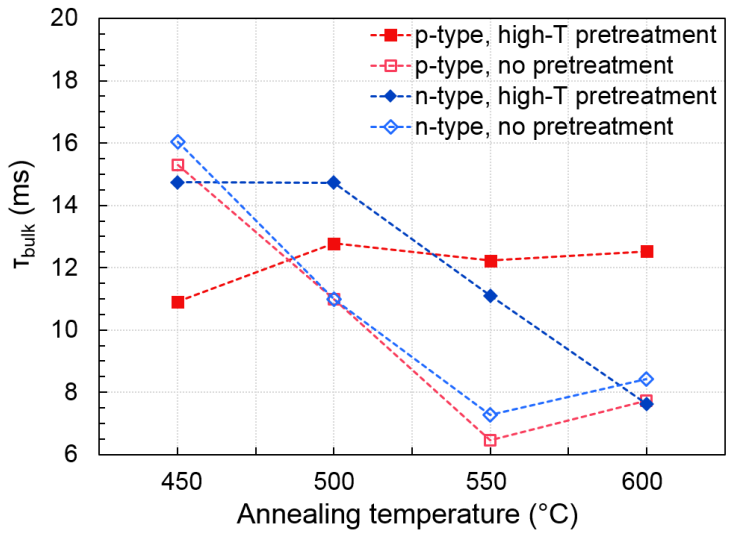

Figure 5. Extracted bulk lifetime for p- and n-type FZ-Si passivated with ALD-Al_2O_3, with and without high-temperature treatment, as function of post-deposition anneal temperature.

Compared to results on low-resistivity substrates, the decrease of bulk lifetimes during post-deposition annealing in substrates of very high resistivity obeys the same trend over temperature, with a minimum in lifetime around 500-550 °C. However, the difference in lifetimes appears to be less compared to low-resistivity substrates: the maximum and minimum lifetimes in the temperature range studied here differ only by a factor of ~2, while for substrates with resistivity < 10 Ωcm, the decrease is more than two orders of magnitude.[21,22] In the same publications, less pronounced lifetime reduction has also been shown for >100 Ωcm substrates, but no further explanations for this observation were discussed.

In light of this, our results strongly suggest that doping concentration plays a role in the degradation of FZ silicon bulk lifetimes by a defect appearing in annealing at low temperatures.

The high-temperature treatment retains high bulk lifetimes at a constant level for p-type substrate in a similar fashion as reported earlier for lower-resistivity FZ silicon, even though its initial bulk lifetime at 450 °C is lower than for the corresponding n-type sample. Interestingly, for the n-type substrates, high bulk lifetimes are only retained up to 500 °C, after which they start to decrease, eventually dropping to the same level with samples without high-temperature treatment. Even though our results may not be directly comparable to the literature in terms of effective lifetimes, as the samples in this work may have experienced additional defect passivation by hydrogen diffusing from the ALD Al_2O_3 film during annealing, the comparison of high-resistivity n- and p-type samples with identical passivation also indicates that the doping species, not only concentration, impacts the curing of the FZ bulk defect. Further studies are required to elucidate the mechanism of defect formation and annealing with doping type and concentration, as well as possible interactions with other impurities, such as nitrogen.

Due to the presence of the FZ-Si bulk defect, a high-temperature step should be included in the device processing flow before any anneal that falls into the 400-800 °C temperature range. In a device using SiO_2 as insulator, this takes place during the oxidation step, and even if a different insulator such as Al_2O_3 is used, the process flow may include an oxidation at >1000 °C, e.g. for growing a hard mask oxide for ion implantation. Our results indicate that to avoid losses in bulk charge carrier lifetimes in n-type samples, any lower-temperature annealing steps should not exceed 500 °C, regardless of previous high-T treatments. In general, the use of lifetime reference samples before or during device processing is an effective way for monitoring the effect of process steps on the surface passivation.

Care should still be taken in the choice of parameters for examining surface passivation quality to take into account the possible changes in the silicon bulk, for example in the case of $S_{eff,max}$ when assuming infinite or constant bulk lifetime. Modeling of different lifetime components can serve as a valuable tool in the separation of bulk and surface effects on effective lifetimes components, although precise identification of defect levels and their assignment to bulk or surface requires further detailed investigation.

4. Conclusions

We demonstrated that Al_2O_3 grown by ALD provides superior passivation compared to thermal SiO_2 on high-resistivity n- and p-type substrates suitable for detector applications. Further inspection on the post-deposition activation anneal of the Al_2O_3 thin film confirmed that temperatures up to 450-500 °C, which are commonly used to sinter the contact metallization in detector fabrication, were suitable to activate the Al_2O_3 passivation on high-resistivity substrates. The total oxide charge of the deposited Al_2O_3 films was highly negative (~1-3×10^{12} cm^{-2}). Even though the charge increased with increasing post-deposition anneal temperature, at higher temperatures effective carrier lifetimes in the Si substrate were limited by a larger number of defect states at the Al_2O_3 film-substrate interface, increasing from (2-4)×10^{11} to >1×10^{12} cm^{-2} eV^{-1}. These observations are in agreement with literature based on low-resistivity substrates, when Al_2O_3 was deposited by thermal ALD, showing that more than substrate resistivity, the passivation characteristics are determined by ALD process parameters and post-anneal. It is concluded that advances on the surface passivation of low-resistivity substrates can be transferred well also to high-resistivity silicon.

A similar lifetime-degrading phenomenon as has been demonstrated for low-resistivity FZ-Si, setting on at post-anneal temperatures starting from approximately 450 °C, appeared to be also present in our high-resistivity samples. We observed that, just as proposed earlier for lower-resistivity samples, a high-temperature treatment prior to ALD did indeed retain bulk lifetimes at a high level for high resistivity p-type silicon. However, in n-type samples, bulk lifetimes were degraded despite this thermal treatment. This indicates that the recombination-active defect, or the mechanism of its deactivation during high-temperature treatment, is influenced – but not exclusively caused – by the dopant species. This connection to the dopant is further supported by the concurring observations in this study and earlier publications showing that the bulk lifetime degradation in FZ silicon is less severe in substrates with higher resistivity, i.e. lower doping concentration. Further research on the nature of this defect, specifically its relation to doping species and concentration, should be conducted.

Acknowledgements

The authors acknowledge the provision of facilities and technical support for sample fabrication and characterization by Micronova Nanofabrication Centre in Espoo, Finland, within the OtaNano research infrastructure at Aalto University. J. Ott would like to thank the Vilho, Yrjö and Kalle Väisälä Foundation of the Finnish Academy of Science and letters for financial support. T. P. Pasanen acknowledges the Aalto ELEC Doctoral School, Jenny and Antti Wihuri Foundation, Walter Ahlström Foundation, and the Foundation of Electronic Engineers for the financial support. Dr. Nitin Nampalli and Mr. Michael Serué are thanked for their help with injection-dependent lifetime modelling.

Received: ((will be filled in by the editorial staff))
Revised: ((will be filled in by the editorial staff))
Published online: ((will be filled in by the editorial staff))

References

[1] A. Ruzin, G. Casse, M. Glaser, A. Zanet, F. Lemeilleur, S. Watts, *IEEE Trans. Nucl. Sci.* **1999**, *46*, 1310

[2] J. Härkönen, E. Tuovinen, P. Luukka, H.K. Nordlund, E. Tuominen, *Nucl. Instrum. Methods Phys. Res. A* **2007***, 579,* 648

[3] M. Ferrero, R. Arcidiacono, M. Barozzi, M. Boscardin, N. Cartiglia, G.F. DallaBetta, Z. Galloway, M. Mandurrino, S. Mazza, G. Paternoster, F. Ficorella, L. Pancheri, H.F-W. Sadrozinski, F. Siviero, V. Sola, A. Staiano, A. Seiden, M. Tornago, Y. Zhao, *Nucl. Instrum. Methods Phys. Res. A* **2019***, 919,* 16

[4] J. Lindroos, H. Savin, *Sol. Energy Mater. Sol. Cells* **2016**, *147*, 115

[5] F. Hartmann, *Evolution of Silicon Sensor Technology in Particle Physics*, Springer International Publishing AG, Cham, Switzerland **2017**

[6] G.F. Knoll, *Radiation Detection and Measurement*, Wiley, Hoboken, NJ, USA **2010**

[7] G. Lutz, *Nucl. Instrum. Methods Phys. Res. A* **1995**, *828*, 21

[8] M.J. Kerr, A. Cuevas, *Semicond. Sci. Technol.* **2002**, *17*, 35

[9] B.E. Deal, *J. Electrochem. Soc.* **1974**, *121*, 198

[10] W. Füssel, M. Schmidt, H. Angermann, G. Mende, H. Flietner, *Nucl. Instrum. Methods Phys. Res. A* **1996,** *377*, 177

[11] B. Hoex, J. J. H. Gielis, M. C. M. van de Sanden, W. M. M. Kessels, *J. Appl. Phys.* **2008**, *104*, 113703

[12] F. Werner, B. Veith, D. Zielke, L. Kühnemund, C. Tegenkamp, M. Seibt, R. Brendel, J. Schmidt, *J. Appl. Phys.* **2011**, *109*, 113701

[13] B. Hoex, S.B.S. Heil, E. Langereis, M.C.M. van de Sanden, W.M.M. Kessels, *Appl. Phys. Lett.* **2006**, *89*, 042112

[14] G. Dingemans, R. Seguin, P. Engelhart, M.C.M. van de Sanden, W.M.M. Kessels, *Phys. Status Solidi RRL* **2010**, *4*, 10

[15] G. Dingemans, N.M. Terlinden, D. Pierreux, H.B. Profijt, M.C.M. van de Sanden, W.M.M. Kessels, *Electrochem. Solid-State Lett.*, **2011**, *14*, H1

[16] G. Dingemans, F. Einsele, W. Beyer, M.C.M. van de Sanden, W.M.M. Kessels, *J. Appl. Phys.* **2012**, *111*, 09713

[17] G. Dingemans and W.M.M. Kessels, *J. Vac. Sci. Technol. A* **2012**, *30*, 040802

[18] M.A. Juntunen, J. Heinonen, V. Vähänissi, P. Repo, D. Valluru, H. Savin, *Nat. Photonics* **2016**, *10*, 777

[19] J. Härkönen, E. Tuovinen, P. Luukka, A. Gädda, T. Mäenpää, E. Tuominen, T. Arsenovich, A. Junkes, X. Wu, Z. Li, *Nucl. Instrum. Methods Phys. Res. A* **2016**, *828*, 46

[20] F.E. Rougieux, N.E. Grant, C. Barugkin, D. Macdonald, J.D. Murphy, *IEEE J. Photovoltaics* **2015**, *5*, 495

[21] N.E. Grant, V.P. Markevich, J. Mullins, A.R. Peaker, F. Rougieux, D. Macdonald, *Phys. Status Solidi RRL* **2016**, *10*, 443

[22] N.E. Grant, V.P. Markevich, J. Mullins, A.R. Peaker, F. Rougieux, D. Macdonald, J.D. Murphy, *Phys. Status Solidi A* **2016**, *213*, 2844

[23] S. Li, N. Yang, X. Yuan, C. Liu, X. Ye, H. Li, *Mater. Sci. Semicond. Process.* **2018**, *83*, 171

[24] N. Nampalli, T.H. Fung, S. Wenham, B. Hallam, M. Abbott, *Front. Energy* **2017**, *11*, 4

[25] A. Richter, F. Werner, A. Cuevas, J. Schmidt, S.W. Glunz, *Energy Procedia* **2012**, *27*, 88

[26] A. Richter, S.W. Glunz, F. Werner, J. Schmidt, A. Cuevas, *Phys. Rev. B* **2012**, *86*, 165202

[27] M. Wilson, J. Lagowski, L. Jastrzebski, A. Savtchouk, V. Faifer, *AIP Conference Proceedings*, **2001**, *550*, 220

[28] C. Claeys, E. Simoen, J. Vanhellemont, *J. Phys. (Paris)* **1997**, *7*, 1469

[29] L.J. Geerligs, D. Macdonald, *Prog. Photovolt. Res. Appl*. **2004**, *12*, 309

[30] V. Naumann, M. Otto, R.B. Wehrsporn, M. Werner, C. Hagendorf, *Energy Procedia* **2012**, *27*, 312

[31] V. Naumann, M. Otto, R.B. Wehrsporn, C. Hagendorf, *J. Vac. Sci. Technol. A* **2012**, *30*, 04D106

[32] S.W. Glunz, D. Biro, S. Rein, W. Warta, *J. Appl. Phys.* **1999**, *86*, 683

[33] H. Jin, K.J. Weber, N.C. Dang, W.E. Jellett, *Appl. Phys. Lett.* **2007**, *90*, 262109

[34] R.S. Bonilla, P.R. Wilshaw, *J. Appl. Phys.* **2017**, *121*, 135301

[35] F. Kersten, A. Schmid, S. Bordihn, J.W. Müller, J. Heitmann, *Energy Procedia* **2013**, *38*, 843

[36] A.G. Aberle, S. Glunz, W. Warta, *J. Appl. Phys.* **1992**, *71*, 4222

[37] J. Benick, A. Richter, T.-T.A. Li, N.E. Grant, K.R. McIntosh, Y. Ren, K.J. Weber, M. Hermle, S.W. Glunz, *35th IEEE Photovoltaic Specialists Conference* **2010**, **DOI:**10.1109/PVSC.2010.5614148

[38] D. Suh, W.S. Liang, *Thin Solid Films* **2013**, *539*, 309

[39] R. Katamreddy, R. Inman, G. Jursich, A. Soulet, A. Nicholls, C. Takoudis, *Thin Solid Films* **2007**, *515*, 6931

[40] V. Cimalla, M. Baeumler, L. Kirste, M. Prescher, B. Christian, T. Passow, F. Benkhelifa, F. Bernhardt, G. Eichapfel, M. Himmerlich, S. Krischok, J. Pezoldt, *Mater. Sci. Appl.* **2014**, *5*, 628

[41] Z.-Y. Wang, R.-J. Zhang, H.-L. Lu, X. Chen, Y. Sun, Y. Zhang, Y.-F. Wei, J.-P. Xu, S.-Y. Wang, Y-X. Zheng, L.-Y. Chen, *Nanoscale Res. Lett.* **2015**, *10*, 46

[42] J. Mullins, V.P. Markevich, M. Vaqueiro-Contreras, N.E. Grant, L. Jensen, J. Jablonski, J.D. Murphy, M.P. Halsall, A.R. Peaker, *J. Appl. Phys.* **2018**, *124*, 035701